Title
Genetic Architecture of Insulin Resistance in the Mouse

Journal
Cell Metabolism, 21(2)

ISSN
1550-4131

Authors
Parks, Brian W
Sallam, Tamer
Mehrabian, Margarete
et al.

Publication Date
2015-02-01

DOI
10.1016/j.cmet.2015.01.002

Peer reviewed

HHS Public Access

Author manuscript

Cell Metab. Author manuscript; available in PMC 2016 February 03.

Published in final edited form as:

Cell Metab. 2015 February 3; 21(2): 334–346. doi:10.1016/j.cmet.2015.01.002.

Genetic Architecture of Insulin Resistance in the Mouse

Brian W. Parks[1,2,3,*], **Tamer Sallam**[1,4], **Margarete Mehrabian**[1], **Nikolas Psychogios**[5], **Simon T. Hui**[1], **Frode Norheim**[6], **Lawrence W. Castellani**[1], **Christoph Rau**[1,2], **Calvin Pan**[2], **Jennifer Phun**[7], **Zhenqi Zhou**[7], **Wen-Pin Yang**[8], **Isaac Neuhaus**[8], **Peter S. Gargalovic**[9], **Todd G. Kirchgessner**[9], **Mark Graham**[10], **Richard Lee**[10], **Peter Tontonoz**[4,11], **Robert E. Gerszten**[5], **Andrea L. Hevener**[7], and **Aldons J. Lusis**[1,2,3,*]

[1] Division of Cardiology, Department of Medicine, David Geffen School of Medicine, University of California, Los Angeles, Los Angeles, California, USA

[2] Department Human Genetics, David Geffen School of Medicine, University of California, Los Angeles, Los Angeles, California, USA

[3] Department of Microbiology, Immunology, & Molecular Genetics, University of California, Los Angeles, Los Angeles, California, USA

[4] Department of Pathology and Laboratory Medicine, University of California, Los Angeles, Los Angeles, California, USA

[5] Cardiovascular Research Center and Cardiology Division, Massachusetts General Hospital, Harvard Medical School, Boston, Massachusetts, USA.

[6] Department of Nutrition, Institute of Basic Medical Sciences, Faculty of Medicine, University of Oslo, Oslo, Norway

[7] Division of Endocrinology, Diabetes and Hypertension, David Geffen School of Medicine, University of California, Los Angeles, Los Angeles, California, USA

[8] Department of Applied Genomics, Bristol-Myers Squibb, Princeton, New Jersey, USA

[9]Department of Cardiovascular Drug Discovery, Bristol-Myers Squibb, Princeton, New Jersey, USA

[10] Isis Pharmaceuticals, Carlsbad, CA, USA

[11] Howard Hughes Medical Institute, University of California, Los Angeles, Los Angeles, California, USA

SUMMARY

[*]**Correspondence:** Aldons J. Lusis (jlusis@mednet.ucla.edu) Phone: 310-825-1359 Brian W. Parks (bparks@mednet.ucla.edu) Phone: 310-825-1595.

Insulin Resistance (IR) is a complex trait with multiple genetic and environmental components. Confounded by large differences between the sexes, environment and disease pathology, the genetic basis of IR has been difficult to dissect. Here we examine IR and related traits in a diverse population of more than 100 unique male and female inbred mouse strains after feeding a diet rich in fat and refined carbohydrates. Our results show dramatic variation in IR among strains of mice and widespread differences between sexes that is dependent on genotype. We uncover more than 15 genome-wide significant loci and validate a gene, *Agpat5*, associated with IR. We also integrate plasma metabolite levels and global gene expression from liver and adipose tissue to identify metabolite Quantitative Trait Loci (mQTL) and expression QTL (eQTL), respectively. Our results provide a resource for analysis of interactions between diet, sex and genetic background in IR.

Keywords

Insulin Resistance; Type 2 Diabetes; Genome-Wide Association Study; Mouse Genetics; Metabolomics; Quantitative Trait Loci (QTL); expression QTL (eQTL); Gene-by-Environment Interactions; Obesity

INTRODUCTION

Insulin resistance (IR) is characterized by the failure of tissues to respond appropriately to insulin. Driven by overconsumption of foods rich in fat and refined carbohydrates throughout the world and increasing rates of obesity, IR has become a serious global health problem. IR is an important contributing factor in type 2 diabetes (T2D) and other diseases, including coronary artery disease and fatty liver disease (Bugianesi et al., 2005; Howard et al., 1996). Decades of biochemical and physiological studies have revealed diverse biological mechanisms that contribute to IR ranging from inflammation and endoplasmic reticulum stress to aberrant lipid metabolism and gut microbiota dysbiosis (Johnson and Olefsky, 2013). While there have been significant advances in our understanding of the pathophysiology of IR, how genetic and environmental factors along with sex differences interact in IR remains poorly understood.

Genetic studies in humans have been successful at identifying genetic loci associated with T2D and other related traits, including obesity and plasma lipid levels (Grant et al., 2006; Scott et al., 2012; Sladek et al., 2007; Speliotes et al., 2010; Teslovich et al., 2010). Despite the successes of genome-wide association studies (GWAS) for T2D, there has been limited success in identifying genetic loci associated with IR in non-diabetic populations. One large GWAS including more than 40,000 non-diabetic individuals identified only two genome-wide significant loci associated with homeostatic model assessment of IR (HOMA-IR) (Dupuis et al., 2010). Recent meta-analyses of glycemic indices in more than 100,000 individuals have expanded this number to 19 loci; however, these loci explain only a few percent of the trait variation (Scott et al., 2012).

In humans, males and females differ dramatically in susceptibility to IR, whereby males are more prone to develop IR than females (Geer and Shen, 2009). Sex-specific distributions between visceral and subcutaneous adipose tissue depots as well as gonadal hormones are

believed to be responsible in part for the dramatic sex differences in IR (Shi et al., 2009). Experimentally, females are less susceptible to fatty acid-induced peripheral IR and have increased insulin sensitivity in adipose tissue (Frias et al., 2001; Macotela et al., 2009). Targeted biochemical studies have even demonstrated that metabolic hormones, such as leptin, have distinct biological actions between males and females (Shi et al., 2008). Clearly, complex biological mechanisms contribute to sex differences in IR and our understanding of how genetic variation contributes to these differences between males and females in IR is limited.

Given the limitations of human studies to identify genetic and environmental interactions associated with IR, we sought to utilize a systems genetics approach (Civelek and Lusis, 2014) using a renewable mouse population to explore genetic, sex and diet interactions contributing to IR. We examined IR traits in a population of 100 common inbred strains of mice, termed the Hybrid Mouse Diversity Panel (HMDP), which is capable of high-resolution genome-wide mapping (most loci less than 1 Mb) and systems-level analysis (Bennett et al., 2010; Farber et al., 2011; Orozco et al., 2012; Parks et al., 2013). We fed HMDP mouse strains a high-fat, high-sucrose (HF/HS) diet and assessed IR and related traits, including central obesity and plasma triglyceride levels. Our results reveal strong relationships between IR and central obesity, similar to observations in human populations (Ritchie and Connell, 2007). Our GWAS analyses identify 15 genome-wide significant loci associated with IR and related traits. Many loci are sex-specific, suggesting that unique genetic variants contribute to IR among males and females. We also integrate plasma metabolite profiles and global gene expression from liver and adipose to identify metabolite Quantitative Trait Loci (mQTL) and expression QTL (eQTL), respectively. Our results provide a resource to identify and interrogate gene-trait, gene-metabolite and gene-gene interactions, as well as identify molecular mediators of IR. We demonstrate the utility of the resource by identifying multiple high-confidence candidate genes and validating a gene associated with the development of IR.

RESULTS

Genetic variation in IR and related traits

A key environmental risk factor driving the development of IR in humans throughout the world is increased consumption of foods rich in fat and refined carbohydrates (Malik et al., 2010). To model this environmental condition in mice we fed more than 100 inbred strains of male and female mice (complete list of strains and numbers in **Table S1**) a HF/HS diet (32% kcal from fat and 25% kcal from sucrose) for eight weeks and measured key IR traits, including plasma insulin, plasma glucose, central obesity and plasma triglyceride levels. To determine relative IR across the population we calculated HOMA-IR (Berglund et al., 2008). After eight weeks of HF/HS feeding we observed a 63-fold variation in HOMA-IR among male mice and a 37-fold variation among female mice (**Figure 1A**). For almost all strains of mice, HOMA-IR was higher in males versus their female counterparts (**Figure 1A**). Moreover, HF/HS feeding was important in increasing HOMA-IR when compared to age-matched chow fed mice in both males and females (**Figures 2D and E**). Along with large variations in HOMA-IR, plasma insulin levels varied from 270 to 9,200 pg/mL in male mice

and from 210 to 5,900 pg/mL in female mice (**Figure S1A**). Plasma glucose levels varied from 150 to 500 mg/dL in male mice and 140 to 420 mg/dL in female mice (**Figure S1B**).

In humans, IR is often associated with obesity and particularly adipose accumulation within the visceral cavity, commonly referred to as central obesity (Johnson and Olefsky, 2013). To test this relationship in our mouse population we measured total body fat percentage and three unique fat depots within the visceral cavity in each mouse included in the study. Total body fat percentage exhibited a significant correlation with HOMA-IR in both male mice ($r=0.39$; $p=1.97 \times 10^{-22}$) and female mice ($r=0.51$; $p=1.77 \times 10^{-30}$) (**Figures 1B and F**). Within the visceral body cavity we dissected and weighed the mesenteric fat, gonadal fat and retroperitoneal fat depots. In the mouse, the mesenteric fat pad is the most comparable to central obesity humans (Catalano et al., 2010). In male strains of mice mesenteric fat mass varied from 0.1 grams to 1.6 grams and in females from 0.1 grams to 2.0 grams (**Figure S2A**). For males the mesenteric fat pad showed the strongest correlation with HOMA-IR ($r=0.45$; $p=7.86 \times 10^{-30}$) (**Figure 1C**). Other fat depots within the visceral cavity, including the gonadal and retroperitoneal fat depots, exhibited a modest correlation with HOMA-IR in male mice (**Figures 1D and E**). In contrast to males, all three adipose depots within the viscera were strongly correlated with HOMA-IR in female mice (**Figures 1G, H and I**). Overall, our data demonstrate large variation in IR among males and females and a striking gender difference between males and females that is dependent on genetic background (**Figure 1A**). Similar to observations in human populations we observed a strong correlation between IR and central obesity (mesenteric fat mass) in both males and females (**Figure 1C and G**).

Metabolic characterization of strains exhibiting differences in HOMA-IR

Our HOMA-IR findings suggest profound variation in the development of IR among inbred strains of mice after consuming a HF/HS diet. To validate these findings we performed euglycemic-hyperinsulinemic clamp studies on the prototypical laboratory mouse strain, C57BL/6J as well as two strains of mice with large differences in HOMA-IR: A/J and DBA/2J. The A/J, C57BL/6J, and DBA/2J strains of mice have average HOMA-IR values of 19, 47, and 113, respectively (**Figure 1A**). Consistent with our HOMA-IR findings the rate of exogenous glucose infusion (GIR) required to maintain euglycemia during euglycemic-hyperinsulinemic clamp studies was significantly reduced in DBA/2J mice, by 56% ($p = 0.013$) compared to A/J mice, whereas C57BL/6J mice showed an intermediate GIR (**Figure 2A**). Insulin-stimulated glucose disposal rate (IS-GDR), which primarily reflects skeletal muscle insulin sensitivity, was reduced by 50% ($p = 0.02$) in DBA/2J mice, compared with C57BL/6J and A/J strains which showed similar insulin responsiveness (**Figure 2B**). Insulin-stimulated suppression of hepatic glucose production (HGP) was significantly blunted ($p=0.001$) in DBA/2J mice as compared with A/J mice (**Figure 2C**) and C57BL/6J mice displayed an intermediate phenotype for HGP suppression (**Figure 2C**).

We also performed *ex vivo* analysis of insulin action and observed that the rate of insulin-stimulated 2-deoxyglucose uptake into the soleus muscle was reduced by 93% for DBA/2J compared to A/J (**Figure S3A**). Furthermore, insulin-stimulated *Akt* phosphorylation (**Figure S3B**) and p85 activated IRS1 (**Figure S3C**) was decreased in DBA/2J mice,

indicating decreased muscle insulin sensitivity. Consistent with findings of diminished glucose disposal in DBA/2J mice, total *Glut4* protein was significantly reduced in quadriceps muscle from DBA/2J compared with A/J mice (**Figure S3D**). In addition to performing detailed physiologic and molecular assessment of insulin sensitivity, we performed metabolic chamber monitoring of A/J and DBA/2J mice to identify potential variations in energy expenditure from the two strains of mice. Both activity (**Figure S3E**) and respiratory exchange rate (RER) (**Figure S3F**) were similar between A/J and DBA/2J mice after eight weeks of HF/HS feeding; thus, energy expenditure cannot explain the differences in IR between A/J and DBA/2J. Furthermore, DBA/2J and A/J did not show any overt difference in body fat percentage after 8 weeks of HF/HS feeding, suggesting that obesity is not the cause of the variation in IR between these two strains (**Figure S3G**). Taken together, the euglycemic-hyperinsulinemic clamp and molecular data support our HOMA-IR assessment (**Figure 1A**).

Contribution of sex hormones to variation in IR

We observed a large difference between males and females in HOMA-IR after 8 weeks of HF/HS feeding, whereby females generally remained more insulin-sensitive versus their male counterparts (**Figure 1A**). To understand this difference and assess the importance of gonadally-derived hormones among strains of mice we designed experiments to test the influence of testosterone and estrogen in males and females, respectively. We examined three genetically unique strains of mice (C3H/HeJ, C57BL/6J, DBA/2J) that have different levels of HOMA-IR. In male mice on a chow diet, gonadectomy in male mice improved HOMA-IR in strain C57BL/6J mice, but not C3H/HeJ or DBA/2J mice, indicating that testosterone exhibits gene-sex interactions (**Figure 2D**). Similarly, in male mice fed a HF/HS diet for 8 weeks, gonadectomy improved HOMA-IR only in strain C57BL/6J (**Figure 2D**). In female mice, ovariectomy increased HOMA-IR in all three strains on both chow and HF/HS diet, demonstrating that estrogens provide insulin-sensitizing effects in female mice. Both gonadectomy and ovariectomy influenced body fat percentage, but the results depended on strain and diet (**Figures S4A and S4B**). Overall our studies indicate that estrogens improve IR and may partially explain why we observed lower HOMA-IR among female mice in all the strains of mice we analyzed (**Figure 1A**). This finding is consistent with published reports showing that ovariectomy in rodents and primates accelerates development of insulin resistance (Kumagai et al., 1993; Wagner et al., 1998). Furthermore, our studies indicate that testosterone influences development of IR in a strain-specific manner.

Genome-wide association mapping for IR and related traits

To identify genetic loci and understand the genetic architecture of IR, we performed GWAS analysis with ~200,000 high quality single nucleotide polymorphisms (SNPs) spaced throughout the genome. To account for population structure among the mice we used a linear mixed model. We used a genome-wide significance threshold of 3.46×10^{-6}, which we have determined through permutation and modeling (Bennett et al., 2010). Due to the strong variation between males and females that is dependent on genetic background (**Figures 1A, S1, and S2**), we performed association separately between males and females.

In males, we identified two genome-wide significant loci associated with HOMA-IR on chromosomes 1 and 9 (**Figure 3A and Table 1**). The peak SNP for chromosome 1 (rs32316569; $p = 5.56 \times 10^{-7}$) contains 109 genes within linkage disequilibrium (LD) and we and others have reported associations with metabolic traits within this region (Chen et al., 2008; Machleder et al., 1997; Parks et al., 2013). One potential causal gene within this locus is apolipoprotein AII (*ApoA2*), which has previously been reported to exacerbate IR when over-expressed in transgenic mice (Castellani et al., 2008). The peak SNP at the chromosome 9 locus (rs36804270; $p = 9.63 \times 10^{-7}$) contains 16 genes within LD. In female mice we did not identify any genome-wide significant loci associated with HOMA-IR (**Figure 3B**).

In addition to HOMA-IR we also performed GWAS with related glycemic indices including plasma insulin and glucose levels. In males, two genome-wide significant loci, on chromosomes 1 and 15, respectively (**Figure S5A and Table 1**) were associated with plasma insulin levels. The peak SNP for chromosome 1 (rs31614030; $p= 4.66 \times 10^{-6}$) is the same locus identified with HOMA-IR. The chromosome 15 locus (rs32269281; $p= 2.85 \times 10^{-6}$) has 11 genes within LD. In females we identified one genome-wide significant locus associated with plasma insulin levels, on chromosome 4 (rs27896920; $p= 4.46 \times 10^{-6}$) containing 13 genes within LD (**Figure S5B and Table 1**). In our data HOMA-IR and plasma insulin levels have a correlation of r=0.56 in males and r=0.45 in females which may explain why we observed similar loci in males but not female mice. Plasma glucose levels had one genome-wide significant locus in both males and females (**Figures S5C, S5D and Table 1**). The male-specific chromosome 7 locus (rs3680765; $p=1.52 \times 10^{-7}$) contains 13 genes within LD while the female-specific chromosome 11 locus (rs27001755; $p=3.33 \times 10^{-7}$) contains 8 genes within LD.

We performed association with common traits associated with IR, including central obesity and plasma triglyceride levels (Pouliot et al., 1992). Using the mesenteric fat pad normalized to body weight we identified one genome-wide significant locus in males and four significant loci in females (**Figures 3C, D and Table 1**). Both males and females contained a strong locus on chromosome 7 (rs32000744; Males $p= 2.71 \times 10^{-06}$, Females $p= 8.73 \times 10^{-7}$), suggesting this locus may harbor a genetic variant that influences central obesity irrespective of sex. Female mice contained three more genome-wide significant loci, two on chromosomes 15 (rs32263766; $p=8.53 \times 10^{-7}$ and rs37298722; $p=3.88 \times 10^{-6}$) and one on chromosome 17 (rs33115366; $p=4.14 \times 10^{-6}$). The chromosome 15 locus (rs37298722) in females contained one gene within LD, *Dnahc5*, a dynein protein that is associated with the microtubule-associated motor protein complex. Sequence analysis identified multiple nonsynonymous coding variants among inbred strains of mice for *Dnahc5* (Keane et al., 2011). Mutations in *Dnahc5* have been associated with primary ciliary dyskinesia type 3 (Hornef et al., 2006). While *Dnahc5* has not been directly linked to obesity, influencing ciliary function has been shown to affect obesity traits (Davenport et al., 2007).

Elevations in plasma triglycerides are commonly associated with IR and central obesity (Pouliot et al., 1992). We measured plasma triglyceride levels among the mice included in our study and did not observe a significant correlation with obesity (data not shown). Plasma triglycerides varied from 7 to 160 mg/dL in male mice and from 8 to 168 mg/dL in female

mice (**Figure S2B**). We identified a genome-wide significant locus for plasma triglyceride levels on chromosome 7 in both males (rs31371723; $p=4.64 \times 10^{-7}$) and females (rs33903345; $p=7.94 \times 10^{-12}$) (**Figures 3E, 3F and Table 1**). In females the locus on chromosome 7 associated with both central obesity and plasma levels of triglycerides in female mice (**Figures 3D, 3F and Table 1**). Male mice also shared a genome-wide significant locus at the chromosome 7 locus for central obesity (**Figures 3C, 3E and Table 1**). The co-mapping of central obesity and plasma triglycerides suggests that a common genetic variant influences both of these metabolic traits. In females there was also a significant locus on chromosome 17 (rs33060525; $p=4.18 \times 10^{-6}$) (**Figure 3E and Table 1**). In total, we were able to identify 15 genome-wide significant loci associated with IR and related traits among males and females (**Table 1**).

Systems genetics analysis of global gene-expression

Our GWAS analysis allowed us to identify 5 loci associated with IR and plasma insulin and glucose levels among males and females. To further refine these loci and identify high-confidence candidate genes we measured global gene expression with microarrays in the livers and adipose tissue of HF/HS fed male mice. Performing GWAS with gene expression data allowed us to identify genes that were regulated locally (*cis* eQTL) versus distally (*trans* eQTL) and ultimately pinpoint genes that have strong genetic variation. In the liver of male HF/HS fed mice we identified 4,599 *cis* regulated genes and 6,244 *trans* regulated genes while in adipose tissue we identified 4,440 *cis* regulated genes and 6,812 *trans* regulated genes.

Focusing on the two peak SNPs on chromosomes 1 and 9 significantly associated with HOMA-IR in male mice we investigated genes regulated in *cis* by rs3231659 and rs36804270, respectively. We identified 6 genes in adipose tissue and 3 genes in the liver that showed evidence of significant genetic regulation by rs3231659 on chromosome 1 (**Table S2**). For peak rs36804270 on chromosome 9 we identified 14 genes in adipose tissue and 15 genes in the liver that showed evidence of significant genetic regulation (**Table S2**). For the chromosome 9 locus (**Figures 4A and B**) only one gene, *Acad11*, has both a significant *cis* eQTL (3.3×10^{-4}) regulated by rs36804270 (**Figures 4C, D and S6E**) and is significantly correlated with HOMA-IR (**Figure 4E**). *Acad11* is an acyl-CoA dehydrogenase that can metabolize long chain fatty acids and generate energy through beta oxidation (He et al., 2011) and our studies implicate *Acad11* as a strong candidate for future studies in IR.

In addition to the identification of loci regulating gene expression we correlated liver and adipose gene expression with HOMA-IR. A number of genes within the top 50 most correlated genes have been previously implicated in the pathology of IR (**Tables S3 and S4**). Specifically, the most significantly correlated gene in the liver was *Igfbp2*, which has a strong negative correlation with IR ($r=-0.65$; $p= 2.05 \times 10^{-23}$) (**Figure S6A**). Consistent with this finding, previous experimental studies in mice have shown that *Igfbp2* is an important anti-diabetic gene in the liver (Hedbacker et al., 2010). In both liver and adipose tissue expression of *Irs2* was strongly negatively correlated with HOMA-IR (**Figures S6B and C**). *Irs2* is a key insulin signaling molecule and consistent with this observation genetic deletion of *Irs2* causes IR and diabetes (Withers et al., 1998). Additionally, in adipose tissue

Cebpb was strongly positively correlated with HOMA-IR (**Figure S6D**). *Cebpb* is a transcription factor responsible for diverse biological responses and consistent with our results mice lacking *Cebpb* have greater insulin sensitivity (Wang et al., 2000).

Integration of plasma metabolites

Metabolomic-based approaches have been utilized with great success to identify groups of metabolites that correlate with development of diabetes and related traits (Cheng et al., 2012; Wang et al., 2011). To identify metabolites associated with IR we used a targeted mass spectrometry approach to measure amino acids, amines and other polar metabolites in the plasma of male mice after eight weeks of HF/HS feeding. Correlation analysis with the 47 metabolites identified xanthosine and ADMA/SDMA (Asymmetric Dimethylarginine/ Symmetric Dimethylarginine) to have the strongest correlations to an IR trait, plasma glucose levels (**Figure 5A**). Xanthosine is an intermediate metabolite of purine metabolism that is commonly studied in the pathology of gout, a condition commonly observed in obesity and consumption of diet rich in fat (Choi et al., 2005). Levels of ADMA/SDMA have been observed to correlate with hyperglycemia in humans and our studies confirm this relationship (Palomo et al., 2011).

To identify genetic loci regulating specific metabolites we performed GWAS with individual metabolites. In total we identified 23 genome-wide significant loci for 10 metabolites (**Table S5**). Some metabolite loci contained genes with a known biological link to the specific metabolite. For example, phosphocholine has one genome-wide significant locus at chromosome 2 (rs27441517; $p= 5.04\times 10^{-8}$) containing four phospholipase genes (*Pla2g4b, Pla2g4d Pla2g4e* and *Pla2g4e*) which are known to act predominantly on phosphocholine-containing lipid species to cleave the sn2 fatty acid (**Figure 5B**). Additionally, plasma levels of 2'-deoxyadenosine, an adenosine derivative, mapped to chromosome 12 (rs37817859; $p=2.88 \times 10^{-6}$) (**Figure 5C**). The peak SNP at this locus is within the poly(A) polymerase alpha, *Papola*, which is a key enzyme mediating polyadenylation during mRNA processing.

We also investigated if any metabolites showed significant regulation by peak SNPs associated with HOMA-IR and related traits. The peak SNP on chromosome 9 (rs36804270) associated with HOMA-IR showed a significant ($p=6.7\times10^{-4}$) association with plasma levels of arginine (**Table S2**) Human studies have observed connections between arginine and insulin resistance and our data further confirm this connection (McLaughlin et al., 2006). Some studies have even found beneficial effects of L-arginine supplementation on insulin sensitivity (Piatti et al., 2001). Additionally, there was evidence that the peak SNP on chromosome 9 was also associated with plasma niacinamide levels (**Table S2**). The chromosome 1 peak SNP (rs32316569) was also associated with plasma levels of glycerol and taurine (**Table S2**). Overall, the integration of plasma metabolite data allowed for identification of relationships between IR traits and the identification of genetic loci that contribute to metabolite regulation.

Identification and validation of *Agpat5* as an effector of IR

The recombinant inbred (RI) strains that are part of the HMDP panel (BXA, AXB, BXH, CXB, and BXD) provide significant power for genome-wide association analysis (Bennett et al., 2010). The BXD subset is by far the largest of these RI panel and the BXD set alone provide sufficient power for genome-wide mapping. We have routinely examined this subset of mice for association, since if a genetic variation exists between the strains C57BL/6J and DBA/2J but not between the other RI panels we would lose power by including the other RI sets within the HMDP. One of the significant loci we identified for plasma insulin levels in this analysis of the BXD RI strains is on chromosome 8 (rs13479627; $p= 7.33 \times 10^{-7}$) (**Figures 6A and B**).

Within the chromosome 8 locus, *Agpat5* (1-acylglycerol-3-phosphate O-acyltransferase 5) was identified as a high-confidence candidate gene. Our gene expression data identified *Agpat5* as having a strong *cis* eQTL in both liver and adipose datasets, indicating there is local regulation of *Agpat5* expression (**Figures 6C and 6D**). Furthermore, Agpat5 is the only gene significantly regulated by the peak SNP, rs13479627 (**Figures 6C and S6F**). To test if *Agpat5* is a gene associated with plasma insulin levels and IR we used antisense oligonucleotides (ASOs) to silence *Agpat5* expression *in vivo*. Using specific ASOs against *Agpat5*, we were able to knockdown *Agpat5* expression by more than 70% in both the liver and adipose tissue (**Figures S7A and B**). To determine if *Agpat5* inhibition would improve IR we fed C57BL/6J mice a high-fat diet for 12 weeks and then treated with *Agpat5* ASO or control ASO for 8 weeks. After 8 weeks of treatment with *Agpat5* ASO mice had reduced plasma insulin levels (**Figure S7C**). To determine IR, we performed a glucose tolerance test in mice and found that mice treated with *Agpat5* ASO were able to clear glucose at a higher rate than control-treated mice (**Figure 6D**).

In addition to studies in mice, we also performed studies in rats fed a high-fructose diet for 12 weeks and then treated with *Agpat5* ASO or control ASO for 8 weeks. Consistent with the mice data, *Agpat5* ASO silenced expression in both liver and adipose (**Figures S7D and E**) in rats. Rats treated with *Agpat5* ASO were able to clear glucose significantly more efficiently than control treated rats (**Figure 6E**) and plasma insulin was also reduced (**Figure S7F**).

Agpat5 is a lipid acyltransferase gene that is important in the conversion of lysophosphatidic acid to phosphatidic acid and biochemical studies indicate that *Agpat5* is localized to the mitochondria (Prasad et al., 2011). Altogether our data identify *Agpat5* as a gene associated with plasma insulin levels and IR and our studies validate across two model organisms (mice and rats) that inhibiting *Agpat5* can significantly improve glucose tolerance after high fat or high fructose feeding, respectively.

DISCUSSION

The genetic basis of IR has proved difficult to dissect in humans due to the many confounding factors that can influence its development. Using a mouse population in which environmental factors can be carefully controlled, we show that common mouse strains exhibit striking variation in the development of IR when fed a HF/HS diet for 8 weeks. We

confirmed this variation in IR using euglycemic hyperinsulinemic clamp studies as well as detailed biochemical studies in strains A/J, C57BL/6J, and DBA/2J mice. Our GWAS results identified three genome-wide significant loci associated with HOMA-IR, one of these in the subset of mice including only the BXD RI strains, and more than a dozen significant loci associated with related traits, such as plasma insulin, glucose, triglyceride and central obesity, among male and female strains. Using a systems genetics approach we were able to integrate both global gene expression data from liver and adipose tissues, as well as plasma metabolomics data. Integration of gene expression allowed us to identify high-confidence candidate genes for HOMA-IR loci and to identify genes highly correlated with HOMA-IR. Integrating metabolomics data we were able to perform GWAS and in some cases pinpoint known genes within the metabolite pathway as well as identify a relationship between IR and plasma arginine levels. Finally, we identified and validated *Agpat5* as a gene contributing to IR.

Males and females differ dramatically in IR and the genetic basis of this difference has yet to be explored in detail. Our study is the first to examine sex differences in IR across a broad set of genetic backgrounds in mice. We observed large sex-biased variation in HOMA-IR and other traits, including plasma insulin, glucose and central obesity. In some strains HOMA-IR was more than 10-fold greater in males, whereas in other strains, males and females were identical. This provides clear evidence for gene-by-sex interactions. Our GWAS results failed to identify common loci associated with HOMA-IR between males and females. This is strikingly different from other traits such as food consumption, where the loci observed are nearly identical between sexes (Parks and Lusis, unpublished). Taken together, our findings demonstrate that unique genetic variants in males and females contribute to IR. We investigated the influence of gonadal hormones in male and females in three unique strains of mice and showed that estrogen contributes to insulin sensitivity in females and testosterone exacerbates IR in C57BL/6J mice, but not other strains we tested. In addition to gonadal hormones, sex chromosomes may also contribute to the varied genetic architecture in males and females (Chen et al., 2012). Detailed analysis of the differences between males and females would provide insights into the mechanisms that contribute to this difference in genetic architecture.

An important result from our study is the identification of three genome-wide significant loci for IR. Our ability to detect variants associated with HOMA-IR may be increased for a number of reasons. First, feeding the mice a HF/HS diet promoted the emergence of genomic variants associated with IR. Second, our mice were maintained in a uniform environment, unlike humans, who have diverse environmental settings. Lastly, mice might harbor stronger genetic variants influencing HOMA-IR. In addition to the identification of genetic loci associated with HOMA-IR and plasma insulin and glucose levels, we also identified loci associated with central obesity and plasma triglyceride levels. Central obesity and plasma triglycerides are commonly associated with IR and in females we identified a locus on chromosome 7 associated with both central obesity and plasma triglyceride levels. Central obesity and plasma triglyceride levels are not correlated in our data and the co-mapping of these two traits to the same locus suggest a common genetic variant may contribute to both traits. A locus on chromosome 7 has previously been reported in an F2

cross between strains C57BL/6 and 129S6 to associate with plasma leptin levels; however, our locus is proximal to this locus (Almind et al., 2003).

Using a systems genetics approach we integrated gene expression data to identify loci controlling gene expression in both liver and adipose tissue. We prioritized genes based on *cis* eQTL and coding sequence variants. For both genome-wide significant loci associated with HOMA-IR we were able to identify multiple genes significantly associated with the peak SNP, which indicates local genetic variation. For the chromosome 9 locus, one gene, *Acad11* is a high-confidence gene based on the *cis* eQTL for this gene and the strong negative correlation with HOMA-IR in adipose tissue. *Acad11* is a gene involved in beta oxidation and plays a role in metabolizing fatty acids to provide energy. In addition to a role in white adipose tissue, *Acad11* is highly expressed in brown adipose tissue and our preliminary studies indicated that *Acad11* gene expression is increased after high fat feeding in brown adipose tissue (Parks and Lusis, unpublished data). Brown adipose tissue is metabolically active and studies in mice indicate that brown adipose is important in regulating insulin sensitivity and development of IR (Stanford et al., 2013), thus based upon our findings further functional studies on *Acad11* are warranted.

In addition to integrating gene expression data into our study, we also measured metabolites in the plasma using a targeted mass spectrometry-based approach. We identified both correlations and > 20 genome-wide significant loci associated with specific metabolites. Using GWAS we were able to pinpoint genes involved in their metabolism of specific metabolites, thereby demonstrating the power of our approach to uncover biological pathways and integrate across biological scales. The branched chain amino acids isoleucine, leucine, valine, tyrosine and phenylalanine are often elevated in individuals with IR and these amino acids have been used as predictive indices of diabetes development (Newgard et al., 2009; Wang et al., 2011). In contrast, our analyses did not find evidence for this relationship. This may be due to the limited duration of HF/HS feeding compared with longer feeding required to develop metabolic consequences typically associated with increased branched-chain amino acids in the plasma. Integrating metabolite data we were able to show that plasma arginine levels are associated with a genome-wide significant locus on chromosome 9 associated with HOMA-IR.

Our work provides a resource to identify genes and pathways involved in the development of IR. To validate the resource we identified *Agpat5*, as a high-confidence candidate gene within a locus associated with plasma insulin levels and HOMA-IR in the BXD RI population. We showed that silencing *Agpat5* expression improves insulin-sensitivity in both mice and rats. Our studies are the first to initiate molecular studies with *Agpat5* and our findings suggest an important role in regulating insulin sensitivity. In addition to *Agpat5*, we identify *Acad11* as a high-confidence candidate gene associated with IR. Our study provides a view of gene-diet interactions and the genetic architecture of IR and related traits in a population of common inbred strains of mice.

EXPERIMENTAL PROCEDURES

Animals

All mice were obtained from The Jackson Laboratory and were bred at University of California, Los Angeles to generate mice used in this study. Mice were maintained on a chow diet (Ralston Purina Company) until 8 weeks of age when they were given a high-fat, high-sucrose diet (Research Diets-D12266B) with the following composition: 16.8 % kcal protein, 51.4 % kcal carbohydrate, 31.8 % kcal fat. A complete list of the strains included in our study is included in **Supplemental Table 1**. The animal protocol for the study was approved by the Institutional Care and Use Committee (IACUC) at University of California, Los Angeles. **Gonadectomy and Ovarietomy.** Male and female mouse strains C57BL/6J, C3H/HeJ and DBA/2J were purchased from The Jackson Laboratory (Bar Harbor, ME). Mice were either maintained on a chow diet (Ralston Purina Company) or placed on a high fat/high sucrose diet (Research Diets D12266B) at 8 weeks of age until 16 weeks of age. At 6 weeks of age the mice were gonadectomized under isoflurane anesthesia. Scrotal regions of male mice were bilaterally incised, testes removed and the incisions closed with wound clips. Ovaries of female mice were removed through an incision just below the rib cage. There were four mice per group. The muscle layer was sutured and the incision closed with wound clips. In sham operated control mice, incisions were made and closed as described above. The gonads were briefly manipulated but remained intact.

Body Composition and Visceral Adipose Analyses

Animals were measured for total body fat mass and lean mass by magnetic resonance imaging (MRI) using Bruker Minispec. To assess size of the three major adipose tissue depots within the visceral cavity, the mesenteric, gonadal and retroperitoneal adipose tissues were carefully dissect from each mouse and weighed.

Plasma Insulin, Glucose and Triglycerides

Retro-orbital blood was collected under isoflurane anesthesia after 4 hours of fasting. Plasma insulin, glucose and triglycerides were determined as previously described (Castellani et al., 2008). The homeostatic model assessment of insulin resistance (HOMA-IR) was calculated using the equation [(Glucose × Insulin)/405].

Hyperinsulinemic-euglycemic clamp studies and *ex-vivo* soleus muscle strip glucose uptake

Described in detail in Supplemental Experimental Procedures.

Association Analysis

Genome-wide association of clinical traits, adipose and liver expression data was performed using FaST-LMM which uses a linear mixed model to correct for population structure (Lippert et al., 2011). For detailed methods see Supplemental Experimental Procedures.

RNA isolation and expression profiling

Total RNA from adipose (211 females, 228 males) and liver (206 females, 227 males) tissue was hybridized to Affymetrix HT_MG-430A arrays and scanned using standard Affymetrix protocols. To reduce the chances of spurious association results, RMA normalization was performed after removing all individual probes with SNPs and all probesets containing 8 or more SNP-containing probes, which resulted in 22,416 remaining probesets. To determine the accuracy of our microarray data we test by qPCR the expression of *Aacs* and found a r=0.7 correlation between qPCR and microarray. All microarray data from this study are deposited in the NCBI GEO (http://www.ncbi.nlm.nih.gov/geo/) under the accession number XXX.

Metabolomics

Metabolic profiling of amino acids, biogenic amines, and other polar plasma metabolites were analyzed by LC-MS as previously described (Roberts et al., 2012; Wang et al., 2011). Metabolite concentrations were determined using the standard addition method.

Agpat5 Validation Studies

C57BL/6J male mice were fed a high-fat diet (Harlan Teklad 06414) for 12 weeks and randomized based on body weight and plasma triglyceride levels. Mice were administered Control Antisense Oligonucleotides (ASOs) or Agpat5 ASO (Isis Pharmaceuticals) for 8 weeks. ASOs were administered weekly at 25 mg/kg. Following 8 weeks of ASO treatment plasma was obtained for insulin quantification. Intraperitoneal glucose tolerance tests (IP-GTT) were performed on 6 hour fasted mice with 1g/kg glucose as previously described (Hevener et al., 2007). Male Sprague Dawley rats were fed a high-fructose diet (Harlan Teklad 89247) for 12 weeks and randomized based on plasma insulin and glucose. Rats were then administered subcutaneously control ASOs or Agpat5 ASOs (25mg/kg/week) for 8 weeks. Following 8 weeks of ASO treatment IP-GTT was performed.

Statistics

Unless otherwise noted values presented are expressed as means ± SEM. Statistical analyses were performed using one- and two-way analysis of variance (ANOVA) using R statistical programming. Significance was set at $P < 0.05$.

Supplementary Material

Refer to Web version on PubMed Central for supplementary material.

ACKNOWLEDGEMENTS

This work was supported by National Institutes of Health (NIH) grant to A.J.L (HL28481). B.W.P. was supported in part by a NIH training grant (HD07228) and an NIH Pathway to Independence Award (HL123021). T.S. was supported by American Heart Association Fellowship (13POST17080115). C.D.R. was supported by a NIH training grant (HL69766). P.T. is supported by the Howard Hughes Medical Institute and NIH (DK063491). R.E.G is supported by NIH (DK-HL081572) and an Established Investigator Award from the American Heart Association. A.L.H is supported by the National Institutes of Health (DK06349 and DK089109) and the UCLA Iris Cantor Women's Health Foundation.

REFERENCES

Almind K, Kulkarni RN, Lannon SM, Kahn CR. Identification of interactive loci linked to insulin and leptin in mice with genetic insulin resistance. Diabetes. 2003; 52:1535–1543. [PubMed: 12765967]

Bennett BJ, Farber CR, Orozco L, Kang HM, Ghazalpour A, Siemers N, Neubauer M, Neuhaus I, Yordanova R, Guan B, et al. A high-resolution association mapping panel for the dissection of complex traits in mice. Genome Res. 2010; 20:281–290. [PubMed: 20054062]

Berglund ED, Li CY, Poffenberger G, Ayala JE, Fueger PT, Willis SE, Jewell MM, Powers AC, Wasserman DH. Glucose metabolism in vivo in four commonly used inbred mouse strains. Diabetes. 2008; 57:1790–1799. [PubMed: 18398139]

Bugianesi E, McCullough AJ, Marchesini G. Insulin resistance: a metabolic pathway to chronic liver disease. Hepatology. 2005; 42:987–1000. [PubMed: 16250043]

Castellani LW, Nguyen CN, Charugundla S, Weinstein MM, Doan CX, Blaner WS, Wongsiriroj N, Lusis AJ. Apolipoprotein AII is a regulator of very low density lipoprotein metabolism and insulin resistance. J Biol Chem. 2008; 283:11633–11644. [PubMed: 18160395]

Catalano KJ, Stefanovski D, Bergman RN. Critical role of the mesenteric depot versus other intra-abdominal adipose depots in the development of insulin resistance in young rats. Diabetes. 2010; 59:1416–1423. [PubMed: 20299478]

Chen X, McClusky R, Chen J, Beaven SW, Tontonoz P, Arnold AP, Reue K. The number of x chromosomes causes sex differences in adiposity in mice. PLoS Genet. 2012; 8:e1002709. [PubMed: 22589744]

Chen Y, Zhu J, Lum PY, Yang X, Pinto S, MacNeil DJ, Zhang C, Lamb J, Edwards S, Sieberts SK, et al. Variations in DNA elucidate molecular networks that cause disease. Nature. 2008; 452:429–435. [PubMed: 18344982]

Cheng S, Rhee EP, Larson MG, Lewis GD, McCabe EL, Shen D, Palma MJ, Roberts LD, Dejam A, Souza AL, et al. Metabolite profiling identifies pathways associated with metabolic risk in humans. Circulation. 2012; 125:2222–2231. [PubMed: 22496159]

Choi HK, Mount DB, Reginato AM. Pathogenesis of gout. Ann Intern Med. 2005; 143:499–516. [PubMed: 16204163]

Civelek M, Lusis AJ. Systems genetics approaches to understand complex traits. Nat Rev Genet. 2014; 15:34–48. [PubMed: 24296534]

Davenport JR, Watts AJ, Roper VC, Croyle MJ, van Groen T, Wyss JM, Nagy TR, Kesterson RA, Yoder BK. Disruption of intraflagellar transport in adult mice leads to obesity and slow-onset cystic kidney disease. Curr Biol. 2007; 17:1586–1594. [PubMed: 17825558]

Dupuis J, Langenberg C, Prokopenko I, Saxena R, Soranzo N, Jackson AU, Wheeler E, Glazer NL, Bouatia-Naji N, Gloyn AL, et al. New genetic loci implicated in fasting glucose homeostasis and their impact on type 2 diabetes risk. Nat Genet. 2010; 42:105–116. [PubMed: 20081858]

Farber CR, Bennett BJ, Orozco L, Zou W, Lira A, Kostem E, Kang HM, Furlotte N, Berberyan A, Ghazalpour A, et al. Mouse genome-wide association and systems genetics identify Asxl2 as a regulator of bone mineral density and osteoclastogenesis. PLoS Genet. 2011; 7:e1002038. [PubMed: 21490954]

Frias JP, Macaraeg GB, Ofrecio J, Yu JG, Olefsky JM, Kruszynska YT. Decreased susceptibility to fatty acid-induced peripheral tissue insulin resistance in women. Diabetes. 2001; 50:1344–1350. [PubMed: 11375335]

Geer EB, Shen W. Gender differences in insulin resistance, body composition, and energy balance. Gend Med. 2009; 6(Suppl 1):60–75. [PubMed: 19318219]

Grant SF, Thorleifsson G, Reynisdottir I, Benediktsson R, Manolescu A, Sainz J, Helgason A, Stefansson H, Emilsson V, Helgadottir A, et al. Variant of transcription factor 7-like 2 (TCF7L2) gene confers risk of type 2 diabetes. Nat Genet. 2006; 38:320–323. [PubMed: 16415884]

He M, Pei Z, Mohsen AW, Watkins P, Murdoch G, Van Veldhoven PP, Ensenauer R, Vockley J. Identification and characterization of new long chain acyl-CoA dehydrogenases. Mol Genet Metab. 2011; 102:418–429. [PubMed: 21237683]

Hedbacker K, Birsoy K, Wysocki RW, Asilmaz E, Ahima RS, Farooqi IS, Friedman JM. Antidiabetic effects of IGFBP2, a leptin-regulated gene. Cell Metab. 2010; 11:11–22. [PubMed: 20074524]

Hornef N, Olbrich H, Horvath J, Zariwala MA, Fliegauf M, Loges NT, Wildhaber J, Noone PG, Kennedy M, Antonarakis SE, et al. DNAH5 mutations are a common cause of primary ciliary dyskinesia with outer dynein arm defects. Am J Respir Crit Care Med. 2006; 174:120–126. [PubMed: 16627867]

Howard G, O'Leary DH, Zaccaro D, Haffner S, Rewers M, Hamman R, Selby JV, Saad MF, Savage P, Bergman R. Insulin sensitivity and atherosclerosis. The Insulin Resistance Atherosclerosis Study (IRAS) Investigators. Circulation. 1996; 93:1809–1817. [PubMed: 8635260]

Johnson AM, Olefsky JM. The origins and drivers of insulin resistance. Cell. 2013; 152:673–684. [PubMed: 23415219]

Keane TM, Goodstadt L, Danecek P, White MA, Wong K, Yalcin B, Heger A, Agam A, Slater G, Goodson M, et al. Mouse genomic variation and its effect on phenotypes and gene regulation. Nature. 2011; 477:289–294. [PubMed: 21921910]

Kumagai S, Holmang A, Bjorntorp P. The effects of oestrogen and progesterone on insulin sensitivity in female rats. Acta Physiol Scand. 1993; 149:91–97. [PubMed: 8237427]

Lippert C, Listgarten J, Liu Y, Kadie CM, Davidson RI, Heckerman D. FaST linear mixed models for genome-wide association studies. Nat Methods. 2011; 8:833–835. [PubMed: 21892150]

Machleder D, Ivandic B, Welch C, Castellani L, Reue K, Lusis AJ. Complex genetic control of HDL levels in mice in response to an atherogenic diet. Coordinate regulation of HDL levels and bile acid metabolism. J Clin Invest. 1997; 99:1406–1419. [PubMed: 9077551]

Macotela Y, Boucher J, Tran TT, Kahn CR. Sex and depot differences in adipocyte insulin sensitivity and glucose metabolism. Diabetes. 2009; 58:803–812. [PubMed: 19136652]

Malik VS, Popkin BM, Bray GA, Despres JP, Hu FB. Sugar-sweetened beverages, obesity, type 2 diabetes mellitus, and cardiovascular disease risk. Circulation. 2010; 121:1356–1364. [PubMed: 20308626]

McLaughlin T, Stuhlinger M, Lamendola C, Abbasi F, Bialek J, Reaven GM, Tsao PS. Plasma asymmetric dimethylarginine concentrations are elevated in obese insulin-resistant women and fall with weight loss. J Clin Endocrinol Metab. 2006; 91:1896–1900. [PubMed: 16507636]

Newgard CB, An J, Bain JR, Muehlbauer MJ, Stevens RD, Lien LF, Haqq AM, Shah SH, Arlotto M, Slentz CA, et al. A branched-chain amino acid-related metabolic signature that differentiates obese and lean humans and contributes to insulin resistance. Cell Metab. 2009; 9:311–326. [PubMed: 19356713]

Orozco LD, Bennett BJ, Farber CR, Ghazalpour A, Pan C, Che N, Wen P, Qi HX, Mutukulu A, Siemers N, et al. Unraveling inflammatory responses using systems genetics and gene-environment interactions in macrophages. Cell. 2012; 151:658–670. [PubMed: 23101632]

Palomo I, Contreras A, Alarcon LM, Leiva E, Guzman L, Mujica V, Icaza G, Diaz N, Gonzalez DR, Moore-Carrasco R. Elevated concentration of asymmetric dimethylarginine (ADMA) in individuals with metabolic syndrome. Nitric Oxide. 2011; 24:224–228. [PubMed: 21419857]

Parks BW, Nam E, Org E, Kostem E, Norheim F, Hui ST, Pan C, Civelek M, Rau CD, Bennett BJ, et al. Genetic control of obesity and gut microbiota composition in response to high-fat, high-sucrose diet in mice. Cell Metab. 2013; 17:141–152. [PubMed: 23312289]

Piatti PM, Monti LD, Valsecchi G, Magni F, Setola E, Marchesi F, Galli-Kienle M, Pozza G, Alberti KG. Long-term oral L-arginine administration improves peripheral and hepatic insulin sensitivity in type 2 diabetic patients. Diabetes Care. 2001; 24:875–880. [PubMed: 11347747]

Pouliot MC, Despres JP, Nadeau A, Moorjani S, Prud'Homme D, Lupien PJ, Tremblay A, Bouchard C. Visceral obesity in men. Associations with glucose tolerance, plasma insulin, and lipoprotein levels. Diabetes. 1992; 41:826–834. [PubMed: 1612197]

Prasad SS, Garg A, Agarwal AK. Enzymatic activities of the human AGPAT isoform 3 and isoform 5: localization of AGPAT5 to mitochondria. J Lipid Res. 2011; 52:451–462. [PubMed: 21173190]

Ritchie SA, Connell JM. The link between abdominal obesity, metabolic syndrome and cardiovascular disease. Nutr Metab Cardiovasc Dis. 2007; 17:319–326. [PubMed: 17110092]

Roberts LD, Souza AL, Gerszten RE, Clish CB. Targeted metabolomics. Curr Protoc Mol Biol. 2012; Chapter 30 Unit 30 32 31-24.

Scott RA, Lagou V, Welch RP, Wheeler E, Montasser ME, Luan J, Magi R, Strawbridge RJ, Rehnberg E, Gustafsson S, et al. Large-scale association analyses identify new loci influencing glycemic

traits and provide insight into the underlying biological pathways. Nat Genet. 2012; 44:991–1005. [PubMed: 22885924]

Shi H, Seeley RJ, Clegg DJ. Sexual differences in the control of energy homeostasis. Front Neuroendocrinol. 2009; 30:396–404. [PubMed: 19341761]

Shi H, Strader AD, Sorrell JE, Chambers JB, Woods SC, Seeley RJ. Sexually different actions of leptin in proopiomelanocortin neurons to regulate glucose homeostasis. Am J Physiol Endocrinol Metab. 2008; 294:E630–639. [PubMed: 18171913]

Sladek R, Rocheleau G, Rung J, Dina C, Shen L, Serre D, Boutin P, Vincent D, Belisle A, Hadjadj S, et al. A genome-wide association study identifies novel risk loci for type 2 diabetes. Nature. 2007; 445:881–885. [PubMed: 17293876]

Speliotes EK, Willer CJ, Berndt SI, Monda KL, Thorleifsson G, Jackson AU, Lango Allen H, Lindgren CM, Luan J, Magi R, et al. Association analyses of 249,796 individuals reveal 18 new loci associated with body mass index. Nat Genet. 2010; 42:937–948. [PubMed: 20935630]

Stanford KI, Middelbeek RJ, Townsend KL, An D, Nygaard EB, Hitchcox KM, Markan KR, Nakano K, Hirshman MF, Tseng YH, et al. Brown adipose tissue regulates glucose homeostasis and insulin sensitivity. J Clin Invest. 2013; 123:215–223. [PubMed: 23221344]

Teslovich TM, Musunuru K, Smith AV, Edmondson AC, Stylianou IM, Koseki M, Pirruccello JP, Ripatti S, Chasman DI, Willer CJ, et al. Biological, clinical and population relevance of 95 loci for blood lipids. Nature. 2010; 466:707–713. [PubMed: 20686565]

Wagner JD, Thomas MJ, Williams JK, Zhang L, Greaves KA, Cefalu WT. Insulin sensitivity and cardiovascular risk factors in ovariectomized monkeys with estradiol alone or combined with nomegestrol acetate. J Clin Endocrinol Metab. 1998; 83:896–901. [PubMed: 9506745]

Wang L, Shao J, Muhlenkamp P, Liu S, Klepcyk P, Ren J, Friedman JE. Increased insulin receptor substrate-1 and enhanced skeletal muscle insulin sensitivity in mice lacking CCAAT/enhancer-binding protein beta. J Biol Chem. 2000; 275:14173–14181. [PubMed: 10747954]

Wang TJ, Larson MG, Vasan RS, Cheng S, Rhee EP, McCabe E, Lewis GD, Fox CS, Jacques PF, Fernandez C, et al. Metabolite profiles and the risk of developing diabetes. Nat Med. 2011; 17:448–453. [PubMed: 21423183]

Withers DJ, Gutierrez JS, Towery H, Burks DJ, Ren JM, Previs S, Zhang Y, Bernal D, Pons S, Shulman GI, et al. Disruption of IRS-2 causes type 2 diabetes in mice. Nature. 1998; 391:900–904. [PubMed: 9495343]

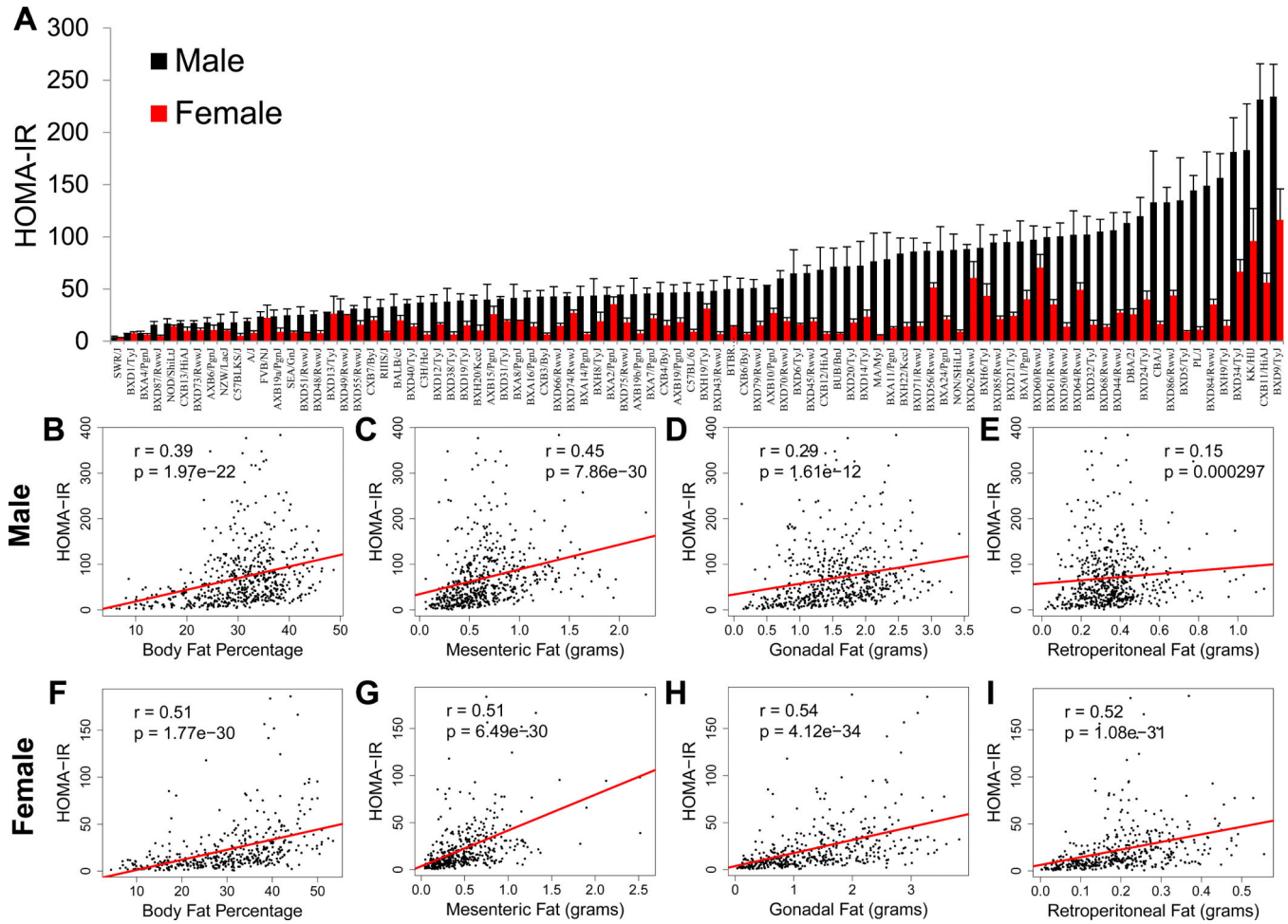

Figure 1. Large genetic variation in insulin resistance among male and female inbred strains of mice

(A) HOMA-IR in male (black) and female (red) mice after 8 weeks of HF/HS feeding. (B-E) Correlation of HOMA-IR with body fat percentage (B), mesenteric fat mass (C), gonadal fat mass (D) and retroperitoneal fat mass (E) in male mice, regression line (red). r, biweight midcorrelation; p, p value.

(F-I) Correlation of HOMA-IR with body fat percentage (F), mesenteric fat mass (G), gonadal fat mass (H) and retroperitoneal fat mass (I) in female mice, regression line (red). r, biweight midcorrelation; p, p value.

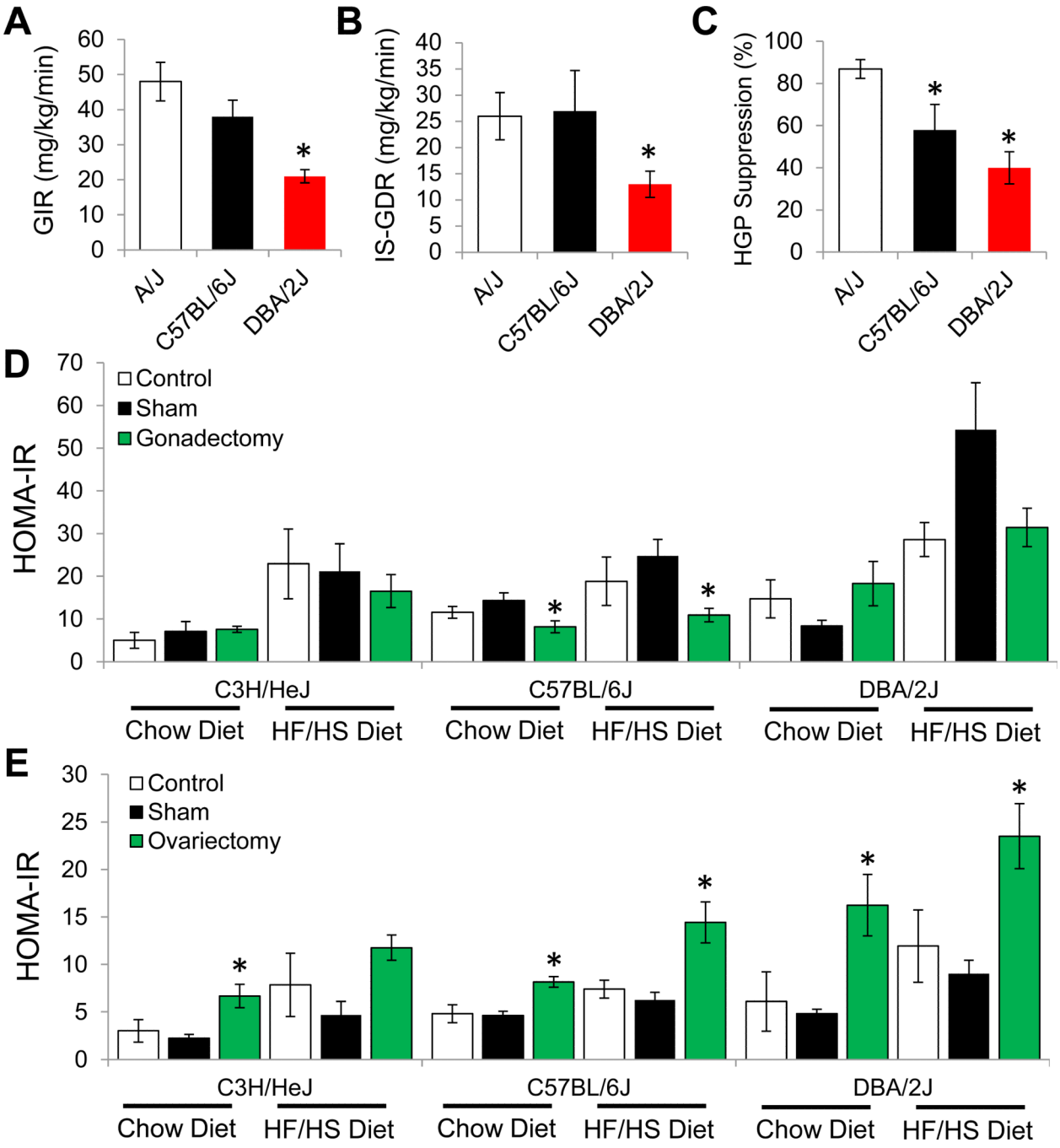

Figure 2. Molecular analysis of IR among strains of mice and role of gonadal hormones in development of IR

(A) Glucose infusion rate (GIR) required to maintain euglycemia during euglycemic hyperinsulinemic clamp studies in A/J, C57BL/6J and DBA/2J mice after 8 weeks of HF/HS feeding.

(B) Skeletal muscle insulin sensitivity represented by the insulin-stimulated glucose disposal rate (IS-GDR) during euglycemic hyperinsulinemic clamp studies in A/J, C57BL/6J and DBA/2J mice after 8 weeks of HF/HS feeding.

(C) Hepatic glucose production (HGP suppression %) during euglycemic hyperinsulinemic clamp studies in A/J, C57BL/6J and DBA/2J mice after 8 weeks of HF/HS feeding.
(D) HOMA-IR in male C3H/HeJ, C57BL/6J and DBA/2J mice after gonadectomy, Sham or control and being maintained on a chow or HF/HS diet for 8 weeks.
(E) HOMA-IR in female C3H/HeJ, C57BL/6J and DBA/2J mice after ovariectomy, Sham or control and being maintained on a chow or HF/HS diet for 8 weeks. Asterisk (*) indicates significance of $p < 0.05$. Error bars represent SEM.

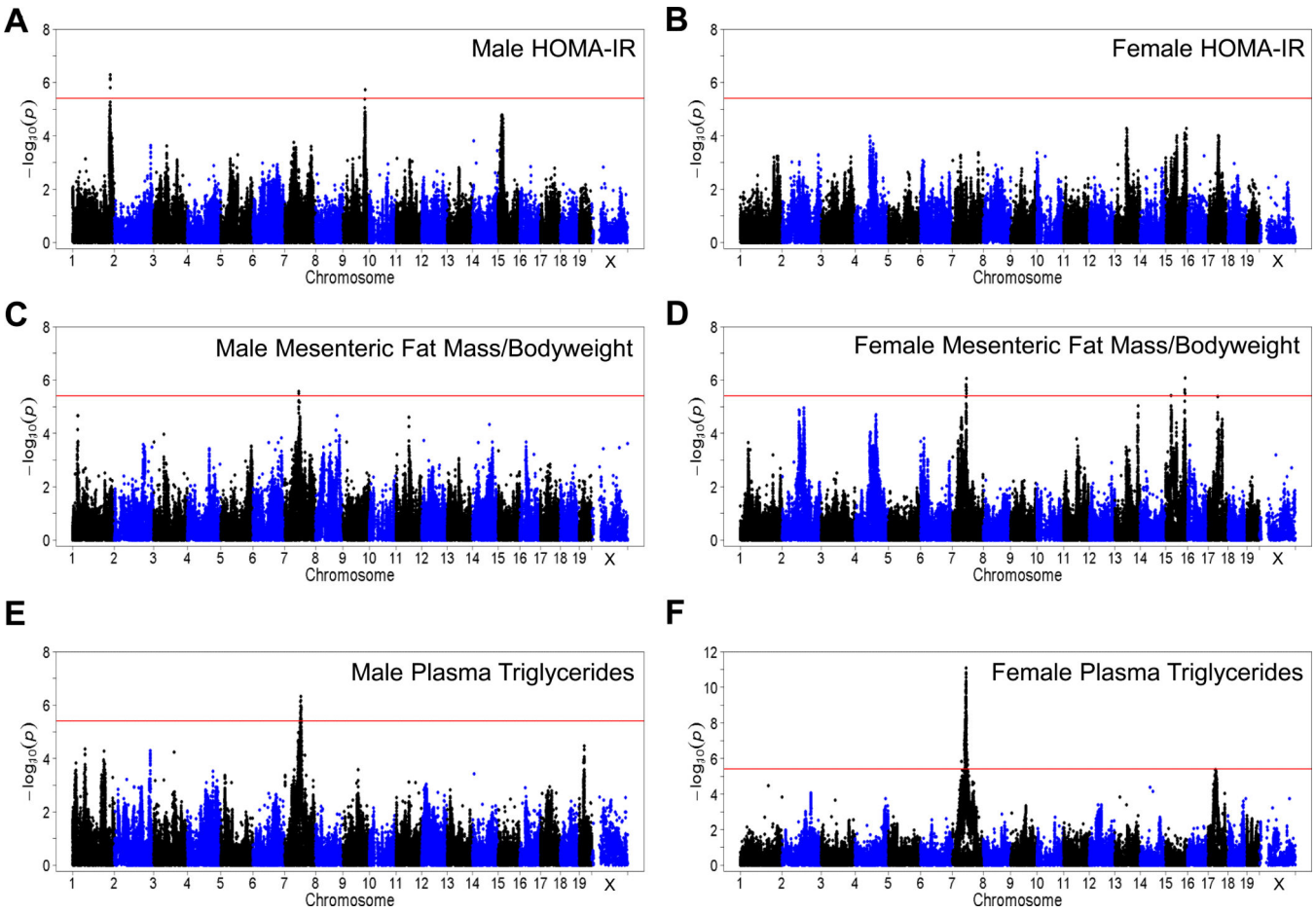

Figure 3. Widespread genetic control of IR and related traits

(A-B) Manhattan plot showing the significance (–log10 of p) of all SNPs and HOMA-IR after 8 weeks of HF/HS feeding in male mice (A) and female mice (B).

(C-D) Manhattan plot showing the significance (–log10 of p) of all SNPs and mesenteric fat mass normalized to bodyweight after 8 weeks of HF/HS feeding in male mice (C) and female mice (D).

(E-F) Manhattan plot showing the significance (–log10 of p) of all SNPs and plasma triglyceride levels after 8 weeks of HF/HS feeding in male mice (E) and female mice (F).

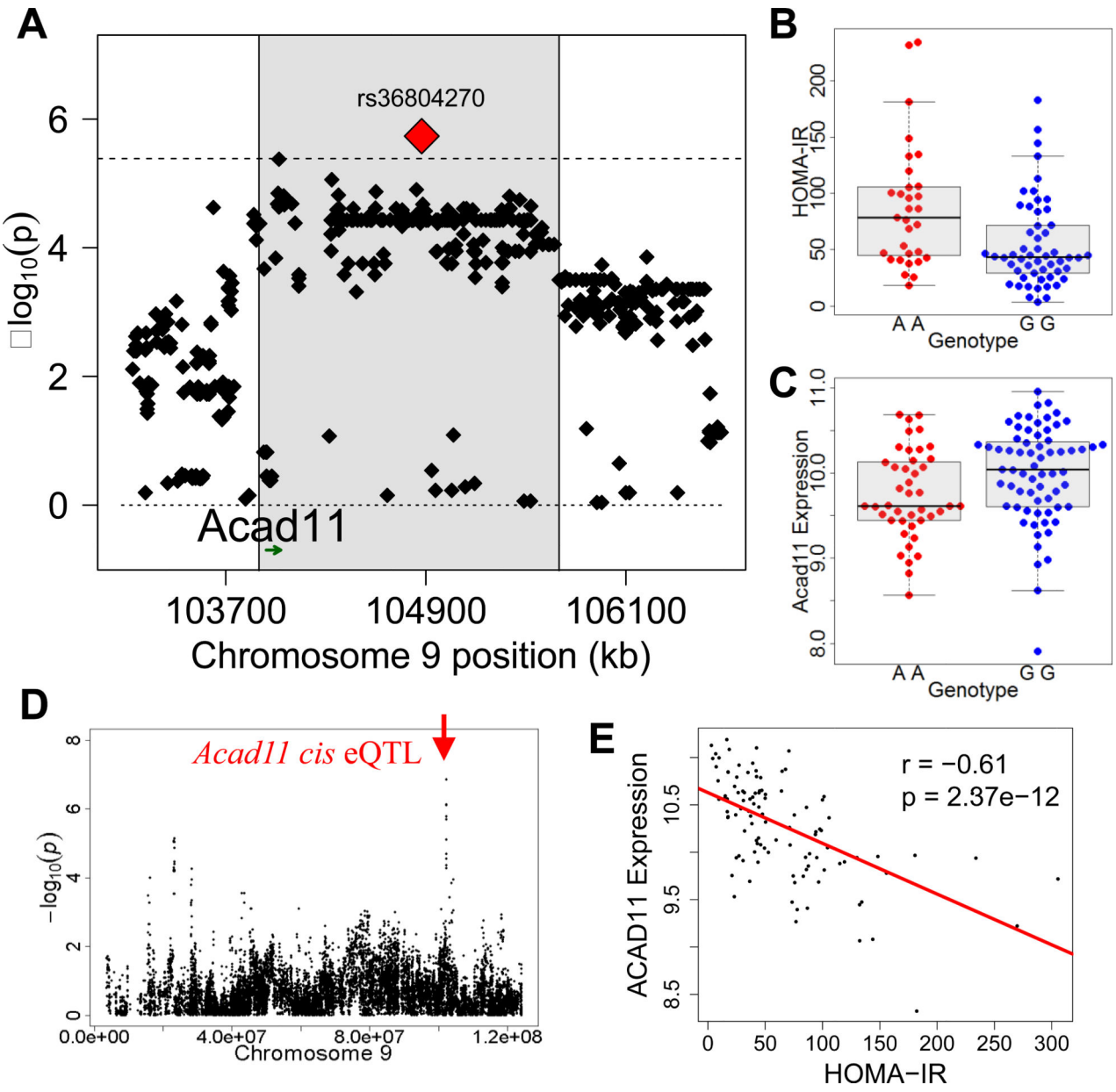

Figure 4. Systems genetics analysis of HOMA-IR

(A) Locus plot for genome-wide significant association with HOMA-IR in male mice at chromosome 9 with approximate LD block (shaded in gray), peak SNP (red) and Acad11 gene position (green). (B) HOMA-IR distribution based on genotype distribution at peak SNP associated with HOMA-IR on chromosome 9 (rs36804270). Box and whisker plot depicting mean and distribution.

(C) *Acad11* adipose expression based on genotype distribution at peak SNP associated with HOMA-IR on chromosome 9 (rs36804270). Box and whisker plot depicting mean and distribution.

(D) Gonadal expression QTL (eQTL) for Acad11 showing (–log10 of p) of all SNPs on chromosome 9 with indicated position of gene (red arrow) of cis eQTL.

(C) Correlation of Acad11 expression in gonadal adipose tissue with HOMA-IR, regression line (red). r, biweight midcorrelation; p, p value.

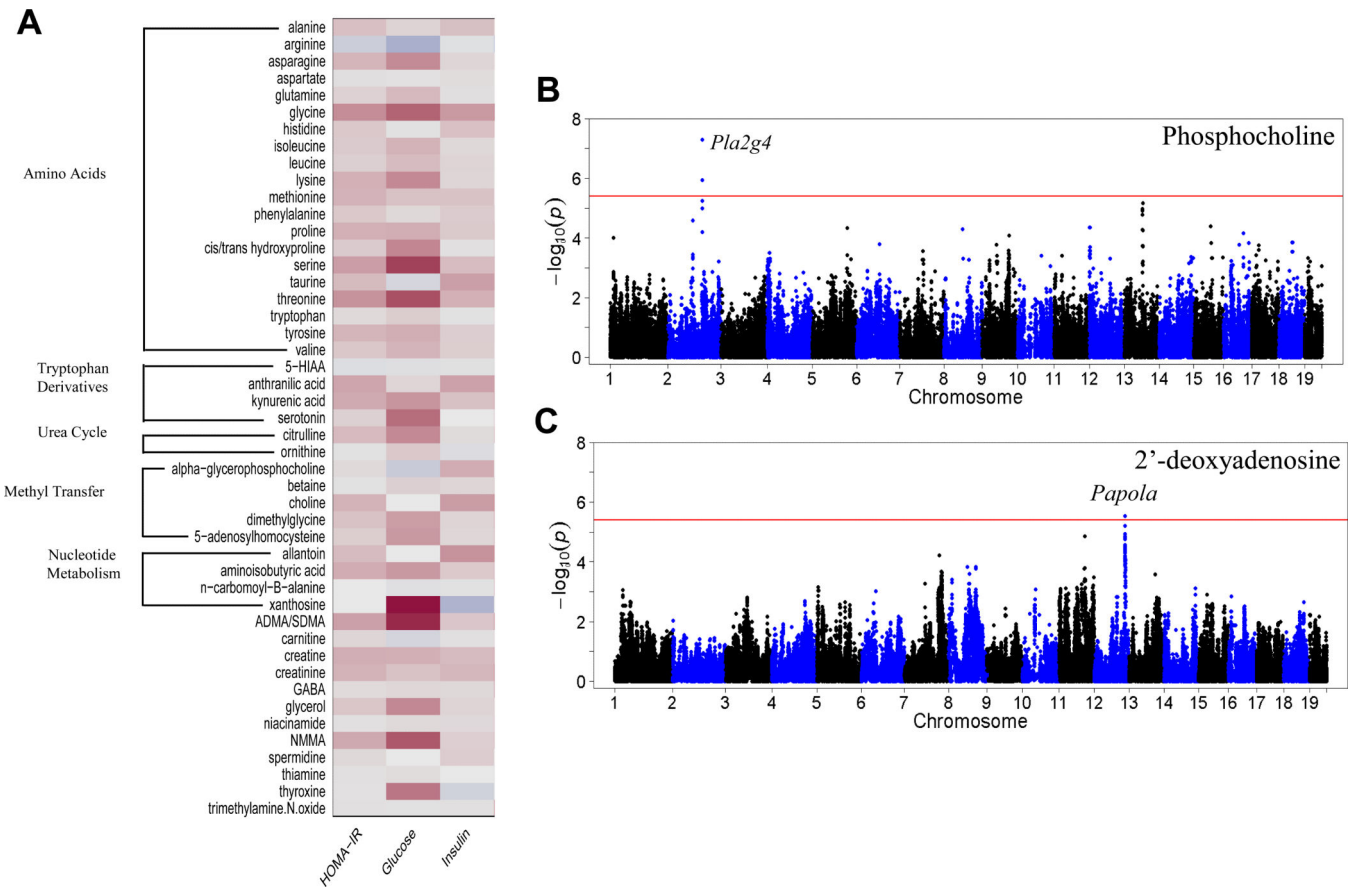

Figure 5. Systems genetics analysis of plasma metabolites

(A) Correlation of plasma metabolites with HOMA-IR, plasma glucose and plasma insulin levels in male mice.

(B) Manhattan plot showing the significance (–log10 of p) of all SNPs and plasma phosphocholine levels after 8 weeks of HF/HS feeding in male mice.

(C) Manhattan plot showing the significance (–log10 of p) of all SNPs and plasma 5'-deoxyadenosine levels after 8 weeks of HF/HS feeding in male mice.

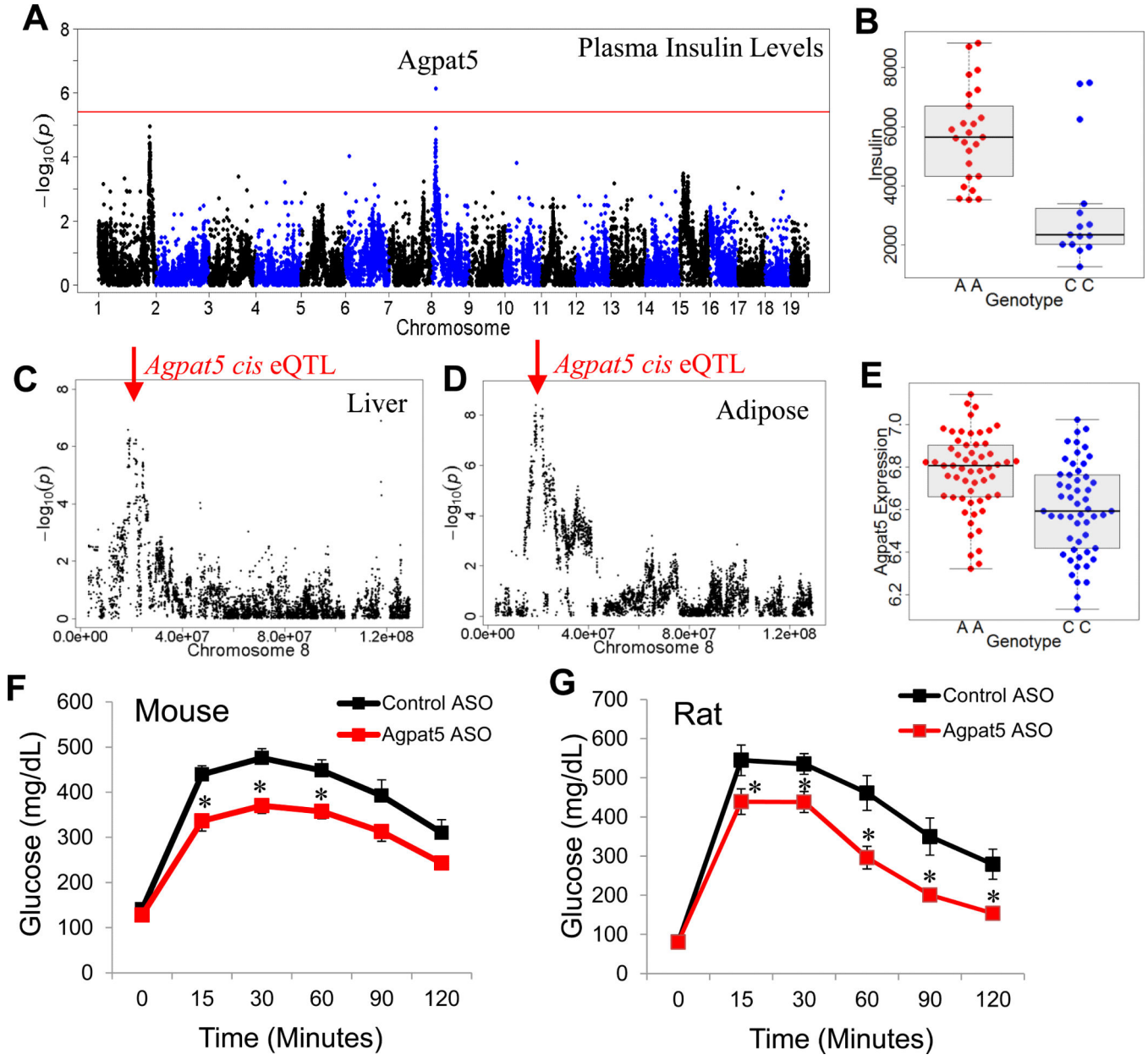

Figure 6. Identification and validation of Agpat5

(A) Manhattan plot showing the significance (–log10 of p) of all SNPs and plasma insulin levels after 8 weeks of HF/HS feeding in male BXD RI strains. Candidate gene for genome-wide significant loci are indicated above genome-wide significant loci

(B) Plasma insulin levels based on genotype distribution at peak SNP associated with plasma insulin levels on chromosome 9 (rs36804270). Box and whisker plot depicting mean and distribution.

(C) Liver expression QTL (eQTL) for Agpat5 showing (–log10 of p) of all SNPs on chromosome 8 with indicated position of gene (red arrow) reflective of cis eQTL.

(D) Gonadal adipose expression QTL (eQTL) for Agpat5 showing (–log10 of p) of all SNPs on chromosome 8 with indicated position of gene (red arrow) reflective of cis eQTL.

(E) *Agpat5* adipose expression based on genotype distribution at peak SNP associated with plasma insulin levels on chromosome 9 (rs36804270). Box and whisker plot depicting mean and distribution.
(F) IP-GTT in C57BL/6J mice fed a high-fat diet for 12 weeks and treated with control ASO or Agpat5 ASO for 8 weeks.
(G) IP-GTT in rats fed a high-fructose diet for 12 weeks and treated with control ASO or Agpat5 ASO for 8 weeks. Asterisk (*) indicates significance of $p < 0.05$. Error bars represent SEM.

Table 1

Genome-wide Significant for Insulin Resistance and Related Traits

Trait	Sex	Chr.	Peak SNP	Position (Mb)	P-Value	MAF	LD	No. of Genes
HOMA-IR	Male	1	rs32316569	175768939	5.22E-07	0.35	175.5-177.4	109
HOMA-IR	Male	9	rs36804270	104875641	1.84E-06	0.36	103.9-105.7	16
Insulin	Male	15	rs32269281	21154862	2.85E-06	0.47	19.0-26.9	11
Insulin	Male	1	rs31614030	173308737	4.66E-06	0.28	172.1-177.4	109
Insulin	Female	4	rs27896920	71287837	4.46E-06	0.33	70.1-75.8	13
Glucose	Male	7	rs3680765	49397123	1.52E-07	0.30	49.0-55.3	13
Glucose	Female	11	rs27001755	112944793	3.33E-07	0.28	112.2-114.6	8
Plasma Triglycerides	Male	7	rs31371723	76638409	4.64E-07	0.28	74.2-79.6	20
Plasma Triglycerides	Female	7	rs33903345	65789990	7.94E-12	0.20	59.0-67.5	38
Plasma Triglycerides	Female	17	rs33060525	35595846	4.18E-06	0.38	35.0-35.9	61
Mesenteric Fat/Bodyweight	Male	7	rs32000744	67559538	2.71E-06	0.45	59.0-67.5	38
Mesenteric Fat/Bodyweight	Female	15	rs32263766	91948444	8.53E-07	0.29	90.9-95.2	22
Mesenteric Fat/Bodyweight	Female	7	rs32000744	67559538	8.73E-07	0.48	59.0-67.5	38
Mesenteric Fat/Bodyweight	Female	15	rs37298722	28527523	3.88E-06	0.30	28.3-29.6	1
Mesenteric Fat/Bodyweight	Female	17	rs33115366	47452733	4.14E-06	0.40	47.4-47.6	6